RESEARCH ARTICLE

A Method for Determining Crude Oil Concentration in Drilling Fluid Based on Laser Raman Spectroscopy Technology

Cunlei Li[1], Chengchi Wang[1], Panpan Chen[1,*], Yawen Jing[2], Dongrui Su[1], Guixin Yu[1] and Mingxuan Li[1]

[1] College of Petroleum Engineering, Liaoning Petrochemical University, Fushun 113001, China
[2] School of Art and Design, Liaoning Petrochemical University, Fushun 113001, China

Abstract

Laser Raman spectroscopy is a promising technique for real-time oil and gas detection in drilling fluids during drilling operations; however, the distribution of crude oil and its coupling with Raman spectral responses under varying temperature conditions remain insufficiently understood, which limits its quantitative applications in downhole environments. This study investigates the temperature- and concentration-dependent behavior of crude oil in oil-containing drilling fluids and develops a quantitative analytical method based on Raman spectroscopy for geological guidance. Crude oil is modeled as dispersed droplets within a continuous fluid phase, and Raman spectra are collected under different temperature and concentration conditions to establish a quantitative relationship between spectral intensity and crude oil concentration. Results show that crude oil exists as dispersed droplets whose size decreases with increasing temperature, accompanied by an increase in interfacial visibility, while higher concentrations lead to a more uniform volume distribution at constant temperature. Raman shifts within 1000–3000cm^{-1} effectively characterize crude oil, with a dominant peak at 1519cm^{-1}, and a positive correlation between peak intensity and crude oil concentration is observed, particularly at elevated temperatures. Based on this relationship, a quantitative model for crude oil detection is established. The proposed method enables accurate real-time identification of oil-bearing formations with minimal influence from concentration variation or formation thickness, providing theoretical support and practical guidance for the application of Raman spectroscopy in LWD systems and improving drilling precision and reservoir evaluation efficiency.

Keywords: logging-while-drilling, oil-containing drilling fluid, raman spectrum, visual ratio, linear equation.

Submitted: 16 March 2026
Accepted: 07 April 2026
Published: 15 April 2026

Vol. 2, **No.** 2, 2026.
10.62762/JGEE.2026.666728

***Corresponding author:**
✉ Panpan Chen
chenpanpan@lnpu.edu.cn

Citation
Li, C., Wang, C., Chen, P., Jing, Y., Su, D., Yu, G., & Li, M. (2026). A Method for Determining Crude Oil Concentration in Drilling Fluid Based on Laser Raman Spectroscopy Technology. *Journal of Geo-Energy and Environment*, 2(2), 118–131.

© 2026 by the Authors. Published by Institute of Central Computation and Knowledge. This is an open access article under the CC BY license (https://creativecommons.org/licenses/by/4.0/).

1 Introduction

Against the backdrop of oil and gas exploration and development advancing toward deep and complex reservoirs, Logging-While-Drilling (LWD) technology serves as the core means to achieve "real-time geological steering", "precise reservoir drilling" and "drilling risk early warning", and its technical advancement directly affects the efficiency and benefits of exploration and development. Currently, LWD technology has been capable of realizing real-time acquisition and transmission of conventional geological parameters such as resistivity, sonic velocity, neutron porosity and density, as well as engineering parameters including weight on bit (WOB), torque, rotational speed, annular pressure and temperature [1–5]. Moreover, wireless LWD, featuring high flexibility and strong adaptability, is gradually replacing wired measurement and occupying a larger share of the LWD market. However, in the key link of LWD—oil and gas mud logging, technical bottlenecks have become increasingly prominent, which has become a crucial factor restricting the efficient development of complex oil and gas reservoirs.

As the detection scenario extends from the ground to the underground, the technical complexity increases exponentially. The harsh downhole conditions such as high temperature, high pressure, and strong drilling fluid disturbance impose extremely high requirements on the stability and anti-interference capability of detection equipment. Currently, to address the problems of complex hydrocarbon system composition and severe spectral overlap in infrared spectroscopy detection technology, the academic community has formed a mature technical route of "pretreatment/feature extraction - modeling analysis". This route optimizes spectral data through methods such as SARA fractionation and net signal analysis, and combines unsupervised learning techniques like principal component analysis (PCA) and hierarchical clustering analysis (HCA), as well as modeling methods including partial least squares discriminant analysis (PLS-DA) and support vector regression (SVR) [6–9] to improve detection accuracy. However, conducting hydrocarbon analysis after pretreatment makes it difficult to meet the real-time requirement [10]; moreover, in reservoirs with low oil content, it is prone to the interference of clay particles and drilling fluid additives on detection results, leading to a significant decline in quantitative accuracy [11]. Against this backdrop, "achieving real-time detection of hydrocarbons in downhole drilling fluid directly without gas-liquid separation" has become the core development direction of LWD oil and gas mud logging technology, and finding detection technologies suitable for this direction has become a key focus of industry research.

The advent of laser Raman spectroscopy technology provides an ideal solution for breaking through the technical bottlenecks in LWD oil and gas mud logging. This technology demonstrates three core advantages in detection: first, it requires no sample pretreatment and is suitable for downhole in-situ detection. Raman spectroscopy enables direct non-contact detection without the need for gas-liquid separation, sample purification and other procedures, which perfectly aligns with the technical trend of "no pretreatment" [12]; second, it possesses robust qualitative and quantitative capabilities as well as excellent anti-interference performance. Hydrocarbon substances exhibit unique Raman characteristic peaks, which allow qualitative identification through peak positions and the establishment of quantitative models via peak intensities. Moreover, it has favorable anti-interference ability against matrix interferences such as water and clay particles in drilling fluid; third, it features high detection speed and stability. The acquisition time of Raman spectra is generally less than 1 minute [13], which can meet the demand for real-time monitoring. Meanwhile, its detection principle is based on molecular vibrational scattering, and the influence laws of downhole environmental factors such as temperature and pressure can be quantified and corrected through experiments, thus showing great potential for engineering application.

Based on the aforementioned background and technical advantages, this study focuses on the core scientific issues and engineering requirements of laser Raman spectroscopy-based hydrocarbon detection while drilling, with specific work centered on experimental simulation and regularity analysis. Firstly, downhole working conditions were simulated in a targeted manner, oil-bearing drilling fluid samples with different oil contents were prepared, and a gradually increasing experimental temperature gradient was set. On one hand, the distribution state of crude oil in drilling fluid was tracked by a microscopic observation system to clarify the mechanism of temperature variation on crude oil dispersion behavior. On the other hand, Raman spectra of oil-bearing drilling fluid samples under the process of temperature rise were collected to analyze the influence law of temperature on spectral characteristics. Finally,

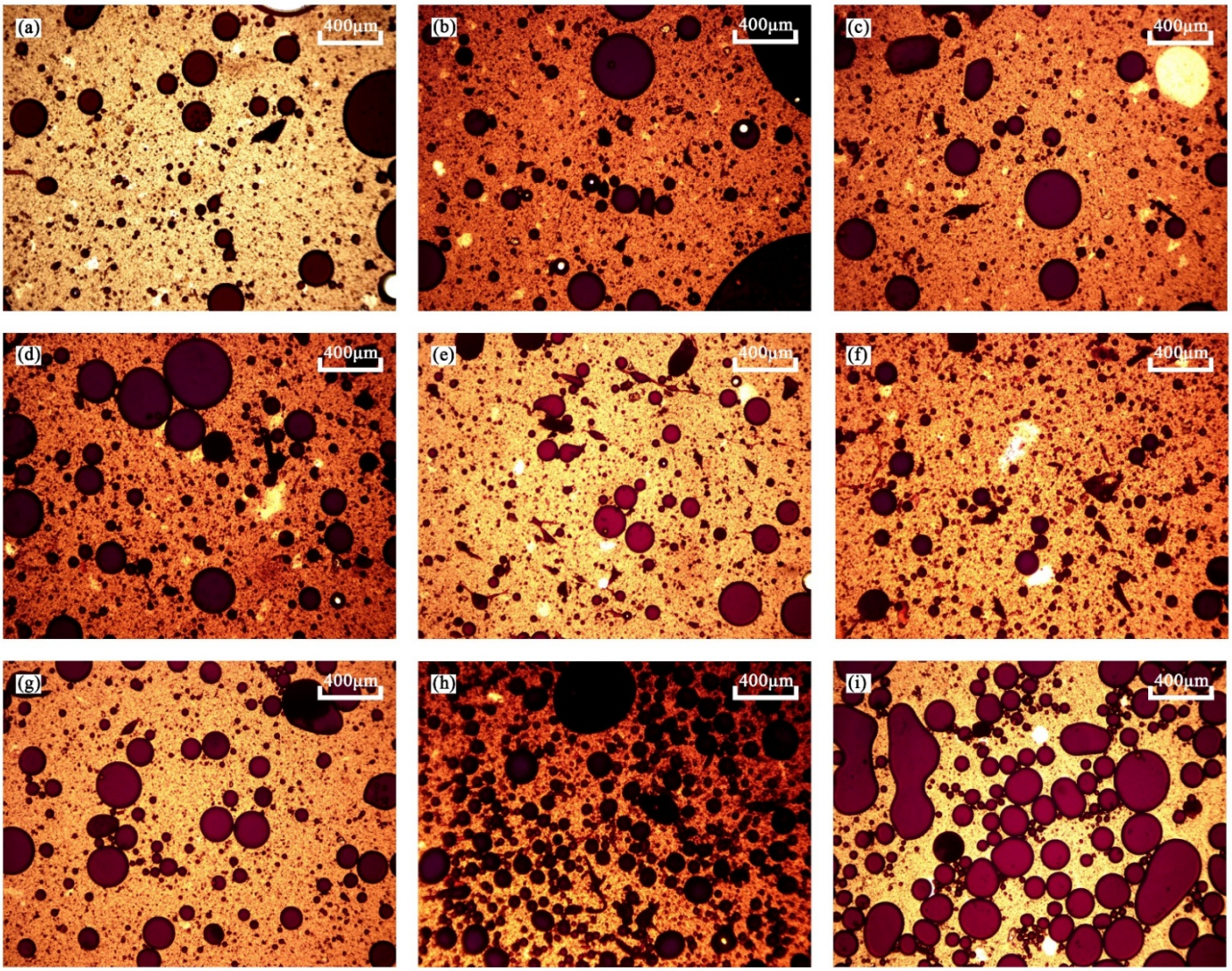

Figure 1. Microscopic Morphology distribution of Oil-bearing Drilling Fluid. (a) Drilling fluid containing 20% crude oil at 35°C; (b) Drilling fluid containing 20% crude oil at 45°C; (c) Drilling fluid containing 20% crude oil at 55°C; (d) Drilling fluid containing 20% crude oil at 65°C; (e) Drilling fluid containing 20% crude oil at 75°C; (f) Drilling fluid containing 20% crude oil at 85°C; (g) Drilling fluid containing 33% crude oil at 85°C; (h) Drilling fluid containing 43% crude oil at 85°C; (i) Drilling fluid containing 50% crude oil at 85°C.

laser Raman spectroscopy was applied for the rapid detection of hydrocarbon content in oil-bearing drilling fluid, providing theoretical basis and experimental support for the further research and development of hydrocarbon detection equipment while drilling.

2 Materials and Methods

The crude oil employed in this experiment was Liaohe crude oil, and a polysulfonate-based drilling fluid was formulated. The micro-morphology of the oil-bearing drilling fluid was observed using a polarizing microscope. For spectral analysis of the oil-bearing drilling fluid, a portable Raman spectrometer (Model SSR-200, manufactured by Nanjing Jianzhi Instrument Equipment Co., Ltd.) was adopted. The key technical parameters of the spectrometer were as follows: spectral resolution $\leq$ 10cm^{-1} @ 1777cm^{-1}; spectral range 150–4300cm^{-1}; detection time 10ms–2min; and laser wavelength 785$\pm$0.5nm.

The experimental procedures for preparing drilling fluids with different crude oil ratios and temperatures were described as follows:

1. Drilling Fluid Preparation: 500mL of drilling fluid was prepared according to the formula (4% bentonite + 0.1% poly anionic cellulose (PAC) + 2% sulfonated phenolic resin type 2 (SMP-2) + 2% sulfonated phenolic nitro humate (SPNH) + 0.4%

ferric chrome lignosulfonate (FCLS)), followed by static curing at room temperature for 24 hours.

2. Equipment Preparation: All experimental apparatus were thoroughly cleaned and dried to ensure internal dryness and freedom from impurities.

3. Crude Oil Pretreatment: 500mL of crude oil was placed in a large beaker and heated in a water bath at 85°C to reduce its viscosity.

4. Preparation of Oil-bearing Drilling Fluid Samples: Aliquots of 40mL drilling fluid were taken separately, and 10mL, 20mL, 30mL, and 40mL of pretreated crude oil were successively added to prepare experimental samples with varying oil contents.

5. Constant-temperature Heating: All samples were placed in a constant-temperature water bath at 35°C and heated for 20minutes to achieve sufficient mixing and temperature equilibrium.

6. Sample Preparation for Microscopic Observation: After heating, the samples were taken out, shaken vigorously to ensure homogeneity, and 20 μL of each sample was pipetted onto a glass slide to prepare observation slides.

7. Polarizing Microscope Observation: The glass slides were placed under a polarizing microscope to observe the distribution state of crude oil in the drilling fluid at the set temperature. The microscopic images were recorded and saved for subsequent analysis.

8. Raman Spectroscopy Detection: The Raman spectrometer was utilized, with the detection probe aligned to the central region of the mixture for measurement. The spectral data of the samples at the corresponding temperature were recorded.

9. Temperature-rising Experiment: The temperature of the constant-temperature water bath was increased stepwise at intervals of 10°C. Steps 5 to 8 were repeated until the temperature reached 85°C. The maximum experimental temperature was set to 85°C with reference to the geothermal gradient rule (a temperature increase of 3°C per 100 meters of depth), to ensure the safety of experimental operations.

3 Results

3.1 Morphological Characteristics of Crude Oil Distribution in Oil-bearing Drilling Fluid

After mixing with water-based drilling fluid, crude oil is mainly randomly distributed in the form of oil-in-water (O/W) emulsion in the drilling fluid. Microscopic observations of the prepared oil-bearing drilling fluid samples reveal that when the crude oil accounts for 20% of the oil-bearing drilling fluid, the dispersion degree of oil droplets in the drilling fluid gradually increases with the rise of temperature. A favorable distribution of oil droplets in the drilling fluid is observed when the temperature reaches 65°C, as shown in Figure 1 (a-f).

When the temperature rises to 85°C, large oil droplets break down into small ones, which are relatively uniformly dispersed in the drilling fluid. At this point, the area of oil droplets were statistically classified with the boundaries of $\leq$ 50 μm^2 and $\geq$ 650 μm^2, with an intermediate interval of 200 μm^2. The statistical classification of oil droplet areas at different temperatures is presented in Figure 2, which intuitively indicates that oil droplets exist in the drilling fluid with smaller particle sizes as the temperature increases.

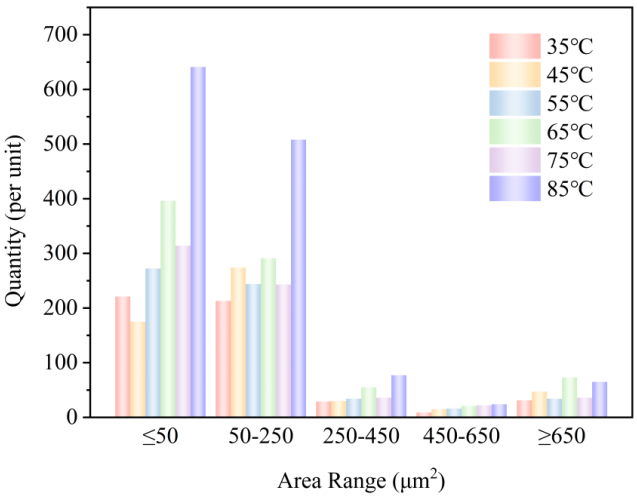

Figure 2. Distribution Intervals of Oil Droplet Area in Drilling Fluid Containing 20% Crude Oil at Different Temperatures.

To simulate the temperature and pressure conditions of crude oil in formations at a depth of 3000m and detect the oil droplet distribution in drilling fluid, oil-bearing drilling fluid samples were prepared in certain proportions to set up control experiments, as shown in Figure 1 (g-i). It can be observed that with the increase in crude oil concentration in the

oil-bearing drilling fluid, the number of oil droplets in the field of view increases accordingly.

Since the above observations were all based on the state of oil-bearing drilling fluid after sample preparation, an identity equation was established following the principle that the total volume of oil droplets in the drilling fluid remains unchanged before and after sample preparation, so as to better simulate the real state of oil droplets in downhole oil-bearing drilling fluid:

$$\pi r^2 h = \frac{4}{3}\pi R^3, \tag{1}$$

where r is the radius of the oil droplet after sample preparation; h is the thickness of the oil droplet after sample preparation; and R is the radius of the oil droplet in the drilling fluid.

During the experiment, a pipette was used to take 20 microliters of drops onto a glass slide, and then it was covered with a cover glass. As the cover glass was a square with a side length of 2cm, the oil droplets would fill the entire cover glass during the slice preparation process (ensuring that the droplets do not overflow the cover glass during the preparation of slices). From this, it can be inferred that the original volume of oil droplets should be equal to the volume under the cover glass at this time:

$$V_{\text{oil-based drilling fluid}} = a^2 h, \tag{2}$$

where a is the side length of the cover glass. According to Equation 2, for the preparation of slices of the oil-containing drilling fluid, the distance between the cover glass and the glass slide is 50μm.

The diameter of the oil droplets can be calculated based on the microscopic photos, and the true volume of the oil droplets can be derived from the microscopic photos by substituting the calculated diameter of the oil droplets into Equation 1. As shown in Figures 1 and 3, the distribution of crude oil are calculated. The radii of all oil droplets in the figure were recorded. According to Equation 1, the volume of oil droplets can be calculated, and based on the distribution of oil droplets at different temperatures, the distribution of oil droplets in the drilling fluid is plotted as shown in Figure 3. It can be seen that the oil droplets are mainly distributed in the range of 1000–5000 μm^3. In the oil-bearing drilling fluid, the oil droplets exist primarily in medium volumes. As the temperature increases, the individual oil droplets become smaller in size but more numerous, resulting in a more uniform and even volume distribution throughout the drilling fluid.

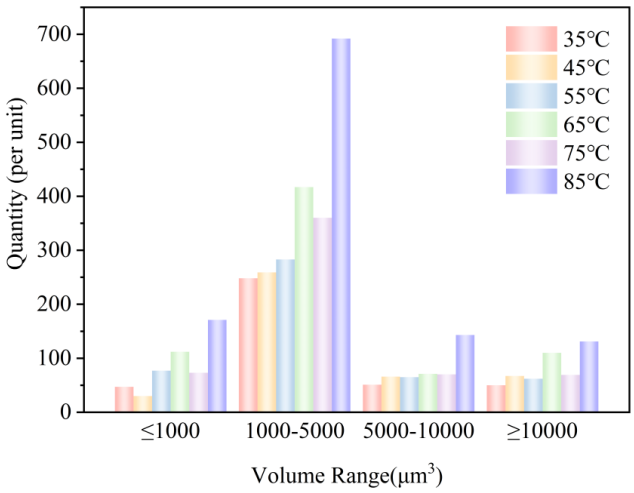

Figure 3. Volume Distribution Profile of Oil Droplets in Drilling Fluid Containing 43% Crude Oil.

3.2 Raman spectrum analysis

3.2.1 *Comparative Raman Spectroscopy of Drilling Fluid, Crude Oil, and Oil-bearing Drilling Fluid*

It can be concluded from the spectrograms that although the alkane structure is determined by carbon-carbon bonds, the number of carbon atoms, carbon-hydrogen bonds and the number of hydrogen atoms, these hydrocarbons exhibit highly similar spectral curves. Constrained by the carbon-carbon skeleton and carbon-hydrogen bonds, these hydrocarbon spectral curves can be categorized into several types corresponding to different alkane classes: n-alkanes, aromatic hydrocarbons, cycloalkanes, etc [14]. Raman spectra are mainly composed of two parts: the fingerprint region and the characteristic region [15]. The fingerprint region of hydrocarbon Raman spectra is primarily located in the low-wavenumber range of 0~1700cm^{-1}, and its spectral features are mainly affected by the vibration of the carbon-carbon skeleton. As this region serves as the fingerprint of the spectrum, the spectral shifts within this range are also referred to as fingerprint peaks. The characteristic region of hydrocarbons is situated in the high-wavenumber range, and its spectral characteristics are mainly dominated by the vibration of carbon-hydrogen bonds. Owing to its role in characterizing specific molecular groups, the spectral shifts in this region are named characteristic peaks. Collectively, fingerprint peaks and characteristic peaks are referred to as Raman peaks or Raman frequency shifts [16].

In the spectral analysis of hydrocarbons, the key characterization parameters for hydrocarbon spectral features are spectral shift and intensity, which can be directly extracted from the spectrograms in this experiment. If the Raman spectrograms are severely affected by noise, spectral processing techniques including fluorescence filtering, data smoothing, wavelet transform and derivative filtering can be applied to obtain clear Raman spectrograms with distinct hydrocarbon characteristic peaks. Subsequently, mathematical models can be established by adopting regression methods such as linear correlation, polynomial regression and exponential regression.

Figure 4 shows the Comparative Raman Spectroscopy of Drilling Fluid, Crude Oil, and Oil-bearing Drilling Fluid with 20% Crude Oil. By locally magnifying the wavenumber range of 1000cm^{-1}~2000cm^{-1}, it can be clearly observed that the peak at the shift of 1519cm^{-1} mainly corresponds to the aromatic ring skeletal stretching vibration of polycyclic aromatic hydrocarbons [17, 18]. This prominent peak appears in all oil-bearing drilling fluid samples with different proportions, playing a decisive role in the Raman-based identification of crude oil during the drilling process.

In the wavenumber range of 2900cm^{-1} ~ 3600cm^{-1}, the characteristic peak of oil-bearing drilling fluid at approximately 3100cm^{-1} is attributed to the C-H stretching vibration of aromatic groups [19]. A particularly distinct peak appears at the wavenumber of 3300cm^{-1} in the drilling fluid spectrum. Given that the drilling fluid prepared in this experiment is water-based, this peak is inferred to originate from the O-H bond vibration [20]. The peaks of oil-bearing drilling fluid in the range of 3000cm^{-1} ~ 3400cm^{-1} exhibit a Raman shift of approximately 100cm^{-1} toward higher values compared with those of pure crude oil. It can thus be deduced that after mixing crude oil with drilling fluid, the lower the crude oil concentration, the greater the Raman shift toward higher values in the range of 3000cm^{-1} ~ 3400cm^{-1}, indicating a stronger interference effect from O-H bonds. In practical detection, the spectral range of 3000cm^{-1} ~ 3600cm^{-1} can serve as a marker for detection and identification, though it is highly susceptible to the influence of crude oil concentration. Overall, the Raman spectrum of crude oil dispersed in drilling fluid is highly consistent with that of pure crude oil, which lays a solid foundation for the quantitative analysis of oil-bearing drilling fluid via Raman spectroscopy.

3.2.2 *Effect of Temperature on Raman Spectra of Oil-bearing Drilling Fluid*

In the Raman spectra of oil-containing drilling fluids with a crude oil concentration of 20% at different temperatures as shown in Figure 5, the peaks in the spectra are not affected by temperature rise. However, the distribution of oil droplets in the drilling fluid affects the Raman spectral peaks. Although temperature has no direct impacts, it indirectly affects the oil droplet area ratio in the field of view in the oil-containing drilling fluid, thereby affecting the Raman spectral peaks.

The Raman spectrum at 1519cm^{-1} Raman shift is zoomed in as shown in Figure 5. When the temperature reaches 45°C and 65°C, the ratios of oil droplets in the field of view are 0.28 and 0.33, respectively. It can be concluded that the Raman spectral peak and oil droplets in the field of view are affected by temperature. As the temperature increases, the oil droplets in the drilling fluid become smaller and more numerous, and Raman irradiation can properly detect the concentration in this case. However, as the temperature continues to rise, the oil droplets become excessively small, such that Raman irradiation of the oil-containing drilling fluid cannot clearly distinguish the oil droplets from the drilling fluid, resulting in a lower Raman peak. Based on the current peak values, the linear relationship between the present Raman relative intensity, temperature and visual area ratio is established (Figure 6).

$$Y_{\text{relative intensity}} = 925.97 + 3958.74x_{\text{visible area ratio}} - 8.15x_{\text{temperature}} \quad (3)$$

3.2.3 *Effect of Crude Oil Concentration on Raman Spectra of Drilling Fluid*

Another objective of this experiment is to simulate the oil and gas contents of formations with different oil-bearing levels and explore the effects of varying oil and gas contents on Raman detection. Raman shifts of spectral peaks reflect molecular structures, while there is a linear relationship between spectral peak intensities and component concentrations. In the experiment, oil-bearing drilling fluid samples with concentrations of 20%, 33%, 43% and 50% were prepared and tested at different temperatures. As can be seen from Figure 7, within the crude oil identification range of 1000 cm^{-1}~3000 cm^{-1}, temperature variations of oil-bearing drilling fluids

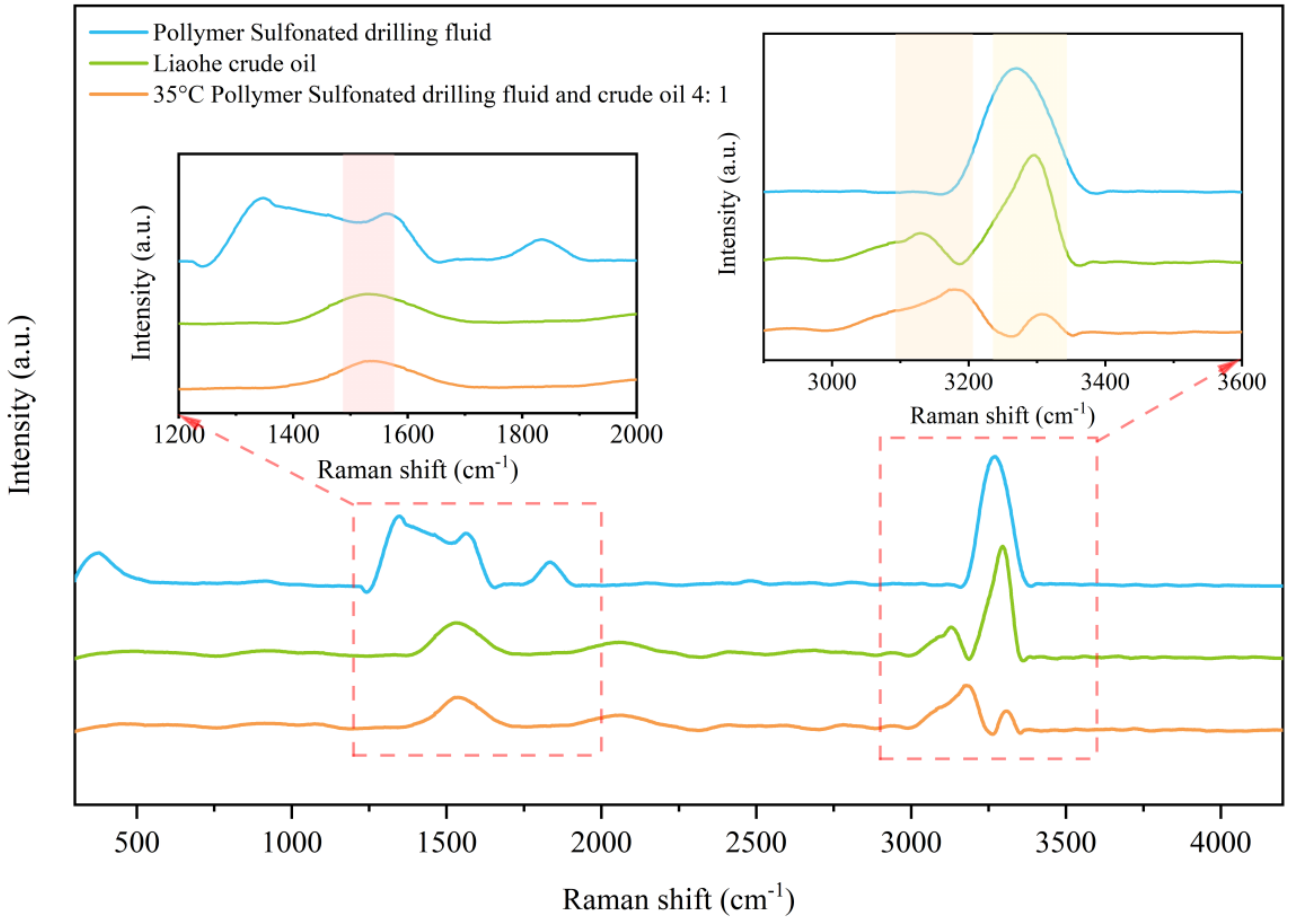

Figure 4. Comparative Raman Spectroscopy of Drilling Fluid, Crude Oil, and Oil-bearing Drilling Fluid with 20% Crude Oil.

will cause fluctuations in the corresponding Raman spectrograms within a certain range.

The peak intensities at the Raman shift of 1519cm^{-1} under different concentrations were further statistically analyzed. As shown in Figure 8, at relatively low temperatures, the crude oil concentration exerts a significant influence on the Raman peak intensity, with the fluctuation range of peak intensities across different concentrations reaching 30 to 100. With the increase of temperature, a positive correlation is observed between the crude oil concentration in the oil-bearing drilling fluid and the Raman peak intensity.

It can thus be concluded that at the same temperature, the higher the concentration of crude oil in the oil-bearing drilling fluid, the higher the corresponding Raman peak intensity. Among the influencing factors, temperature exerts a significant effect on the Raman peak intensities of samples with different concentrations. Under high-temperature conditions, a linear relationship is observed between the crude oil concentration and the Raman peak intensity. Therefore, Raman spectroscopy can be applied for real-time detection of the Raman peak intensity of crude oil in oil-bearing drilling fluid, which is particularly suitable for low-oil reservoirs, thin-layer reservoirs and shallow oil reservoirs.

3.2.4 *Quantitative Identification of Crude Oil Concentration in Oil-bearing Drilling Fluid*

In some practical applications, the types of background components of the sample to be tested are basically unchanged, and the proportion of each background component changes only within a certain range. In this case, the spectral shape of the background component only has a few limited cases [21]. When performing a quantitative analysis, each background spectrum in the background spectrum database could be used as a known quantity for linear weighted stacking with the spectral signal of the component to be measured, resulting in a linear synthesized spectrum. The synthesized spectrum was compared with the measured mixture spectrum. The background line

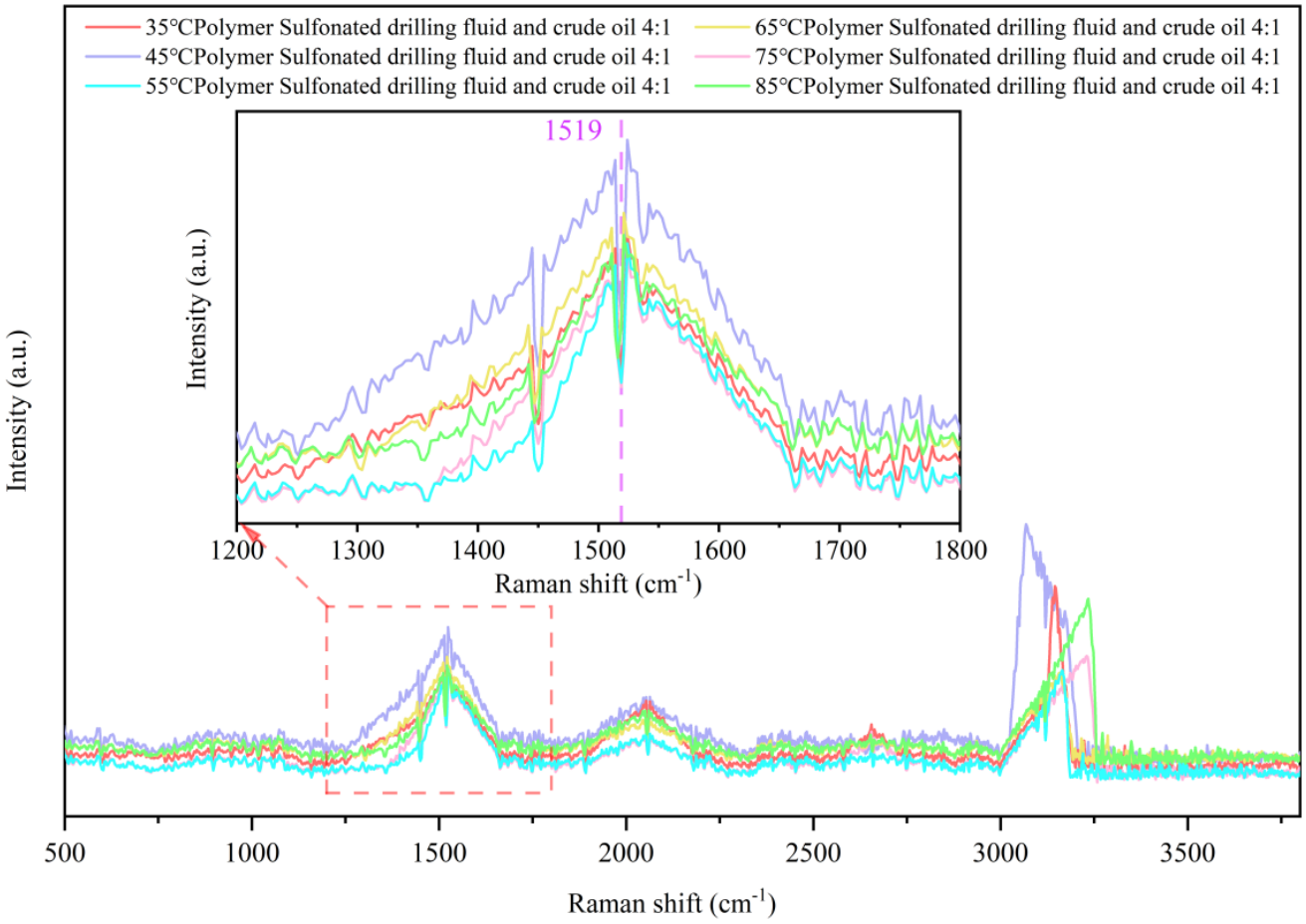

Figure 5. Raman Spectra of Oil-bearing Drilling Fluid with 20% Crude Oil at Different Temperatures.

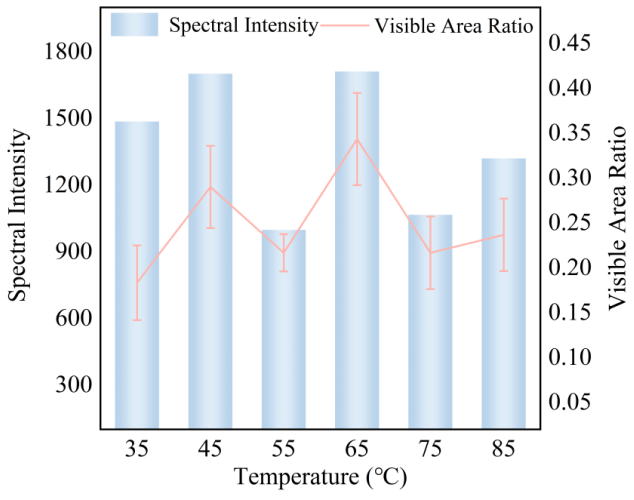

Figure 6. Correlation Diagram of Raman Spectral Intensity and Visual Area at Different Temperatures.

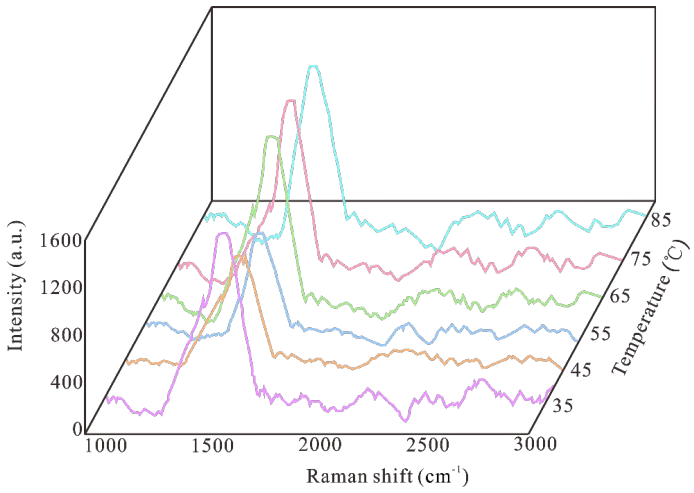

Figure 7. Variation of Raman Spectral Peak Intensities at Different Temperatures in the Wavenumber Range of 1000–3000 cm^{-1}.

corresponding to the synthetic spectrum with the smallest error was used as the known background in the next quantitative analysis [22–25].

3.2.5 Construction of Synthetic Spectrum Model with Known Background Spectrum

During the experiment, the oil-containing drilling fluid was prepared by mixing the crude oil of different

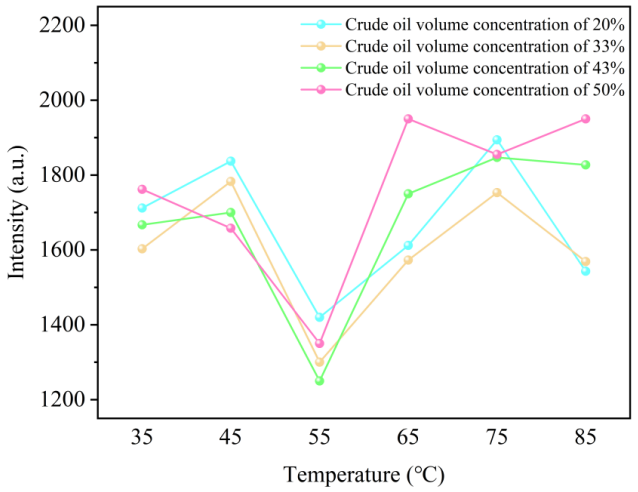

Figure 8. Comparison Plot of Raman Peak Intensities at 1519cm^{-1} Under Different Temperatures.

concentrations with a certain amount of drilling fluid. The crude oil in the oil-containing drilling fluid was used as the substance to be tested. The drilling fluid could be regarded as a background mixture. R_{drilling} represents the Raman spectrum of the background mixture. According to the principle of spectral superposition, it can be concluded that the Raman spectrum R_{mixture} of the oil-bearing drilling fluid should conform to the linear superposition relationship of the crude oil spectrum R_{oil} and the background spectrum R_{drilling}, namely:

$$R_{\text{mixed}}(\nu) = \gamma A_{\text{drilling}} R_{\text{drilling}}(\nu) + x A_{\text{oil}} R_{\text{oil}}(\nu), \quad (4)$$

In this equation, A_{drilling} is the Raman intensity of the background mixture; A_{oil} is the Raman intensity of the component to be measured; ν is the wave number.

Let K_{oil} represent the relative Raman intensity coefficient of the composition to be tested and the background mixture, namely:

$$K_{\text{oil}} = \frac{A_{\text{oil}}}{A_{\text{drilling}}}, \quad (5)$$

As the background substance for the experiment is a laboratory-prepared drilling fluid, K_{oil} is a constant in this case. By substituting Equation (5) into Equation (4), the following expression is obtained:

$$R_{\text{mixed}}(\nu) = A_{\text{drilling}} \left[\gamma R_{\text{drilling}}(\nu) + x K_{\text{oil}} R_{\text{oil}}(\nu)\right], \quad (6)$$

where x and y are the volume components of crude oil and drilling fluid in the oil-containing drilling fluid, respectively.

$$x + y = 1, \quad (7)$$

In order to eliminate the impacts of such factors as the environment and the like on the intensity of the Raman spectrum, the measured oil-containing drilling fluid spectrum was normalized. Let $v_{\text{normalized}}$ represent the normalized wave number, and the normalized spectrum of the oil-containing drilling fluid is obtained as:

$$\begin{aligned}\bar{R}_{\text{mixed}}(v) &= \frac{R_{\text{mixed}}(v)}{R_{\text{mixed}}(v_{\text{normalized}})} \\ &= \frac{(1-x)R_{\text{drilling}}(v) + xK_{\text{oil}}R_{\text{oil}}(v)}{(1-x)R_{\text{drilling}}(v_{\text{normalized}}) + xK_{\text{oil}}R_{\text{oil}}(v_{\text{normalized}})}\end{aligned} \quad (8)$$

Let:

$$a = \frac{1-x}{(1-x)R_{\text{drilling}}(v_{\text{normalized}}) + xK_{\text{oil}}R_{\text{oil}}(v_{\text{normalized}})} \quad (9)$$

$$b = \frac{xK_{\text{oil}}}{(1-x)R_{\text{drilling}}(v_{\text{normalized}}) + xK_{\text{oil}}R_{\text{oil}}(v_{\text{normalized}})} \quad (10)$$

Then the normalized spectrum of the oil-containing drilling fluid can be written as the weighted sum of the drilling fluid and the crude oil to be tested.

$$\bar{R}_{\text{mixed}}(v) = a\bar{R}_{\text{drilling}}(v) + b\bar{R}_{\text{oil}}(v), \quad (11)$$

Taking the oil-bearing drilling fluid with 20% crude oil concentration at 75°C as an example, the corresponding Raman spectrogram was obtained via laser Raman spectroscopy detection, as presented in Figure 9. Based on the aforementioned analysis, it can be determined that oil-bearing drilling fluid and pure crude oil are distinguishable within the wavenumber range around 1500 cm^{-1}. Therefore, this study selected the characteristic peak at the wavenumber of 1519 cm^{-1} of the simulated downhole oil-bearing drilling fluid as the research object. Specifically, the peak intensity of the oil-bearing drilling fluid at 1519 cm^{-1} reached 1724; the peak intensity of the blank drilling fluid at the same wavenumber was 1067; and the peak intensity of pure crude oil at this wavenumber was 1200. These values were substituted into Formula 5-11 for wavenumber normalization, yielding the relational expression for the oil-bearing drilling fluid as follows:

$$\overline{R}_{\text{mixed}}(\nu) = 1.12R_{\text{drilling}}(\nu) + 0.78R_{\text{oil}}(\nu), \quad (8)$$

The synthesis coefficient of the background spectrum and the measured component spectrum in the mixture can be obtained through the spectral synthesis algorithm introduced previously. To

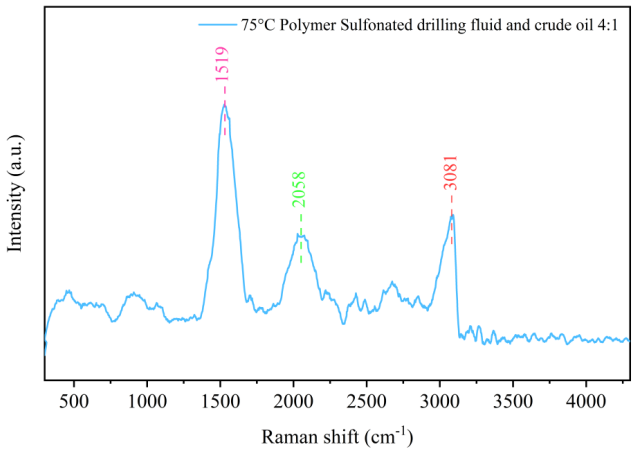

Figure 9. Raman Spectrum of Drilling Fluid Containing 20% Crude Oil at 75°C.

quantitatively analyze the concentrations of the measured components in the mixture, the intensity coefficient K_{oil} of the relative Raman spectrum must also be known. According to Equation 9 and Equation 10, it follows that:

$$K_{\text{oil}} = \left(\frac{b}{a}\right) \times \left(\frac{1-x}{x}\right), \tag{9}$$

$$x = \left(\frac{b}{aK_{\text{oil}} + b}\right), \tag{10}$$

During the analysis and prediction of the concentration of the component to be tested in the unknown sample, the relative Raman intensity coefficient K_{oil} and the spectral synthesis coefficients a, b of the component to be tested and the background mixture were first calculated, and then substituted into the linear model expressed by Equation 14 for the predicted value of the volume component of the component to be tested.

3.2.6 *Validation of the Effectiveness of Quantitative Identification for Crude Oil*

For quantitative analysis, 40mL of drilling fluid was mixed with different volumes of crude oil at 75°C to obtain four mixed samples of oil-bearing drilling fluid. The Raman spectra of crude oil, pure drilling fluid, and oil-bearing drilling fluid were measured, with an integration time of 3s for each sample's Raman spectrum, and the average value was taken from multiple measurements. Due to the presence of strong fluorescence background in the measured spectra, fluorescence removal processing was required for the spectra. In addition, to eliminate the influence of instrument parameters on spectral intensity, normalization processing was performed on oil volume fraction.

In the quantitative analysis of crude oil with known drilling fluid content, according to Formula 13, for the i-th (i=1, 2, 3) type of drilling fluid, only one oil-bearing drilling fluid sample containing this type of drilling fluid was required as a calibration sample to calculate the Raman intensity coefficient K of crude oil and drilling fluid. The synthesis coefficients were calculated via Formula 9 and Formula 10, and a linear regression model between the synthesis coefficients and crude oil concentration was established. The crude oil concentration at this time could be calculated given a fixed volume.

To eliminate the influences of instruments and environment, normalization processing was conducted on the peak intensities of drilling fluid and crude oil. These normalized values were then substituted into Formula 5, Formula 9, Formula 10, and Formula 11. To verify the error range between the calculated values and the actual values, multiple groups of calculations were performed, and the results are shown in Figure 10. It can be observed that the error gradually increases with the rise of crude oil concentration, but the overall error does not exceed 1%. Therefore, the quantitative analysis method proposed in this study can accurately evaluate the crude oil concentration in oil-bearing drilling fluid.

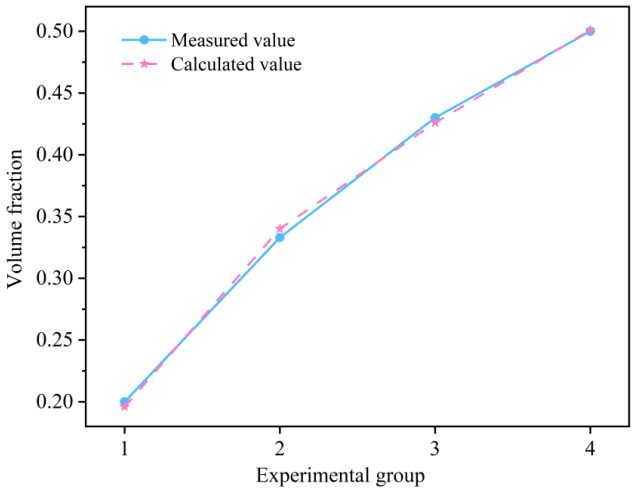

Figure 10. Comparison Plot of Measured vs. Calculated Crude Oil Concentrations in Oil-Bearing Drilling Fluids with Different Concentrations at 75°C.

The above quantitative analysis was performed at the same temperature, but in the actual detection process, the temperature was affected by the formation depth. Raman peaks at different temperatures at the same wavenumber increase with the rise in temperature, and the relationship between temperature and wavelength

is established as follows:

$$R(v)_T = 3.66T + 1595.9 \quad (15)$$

In this equation, T is the temperature, $R(v)_T$ is the wavelength at the temperature T. In order to make the wavelengths at different temperatures more accurate and be less affected by error factors, $R(v)_T$ shall be normalized.

The peaks of Raman spectra of oil-containing drilling fluids at different temperatures could be inferred from Equation 15, normalized, and substituted into the equation for quantitative analysis of the crude oil. On the basis of the analysis of Raman spectral substances and in response to the changes in spectrum of the mixture and the known background spectrum, the mixture spectrum was expressed as a weighted combination of the known background spectrum and the component spectrum to be tested. During the process of calculating the combination coefficient, the parameters of the spectral model of the component to be tested were adjusted to fit the nonlinear changes in the spectrum of the component to be tested. A linear relationship between temperature and Raman spectroscopy was established between temperature and Raman spectroscopy, and normalize the wavelength at a certain temperature to make the results more accurate.

4 Discussion

The present study systematically investigated the distribution characteristics of oil droplets and Raman spectral responses of oil-containing water-based drilling fluids under simulated formation temperatures, and established a temperature-corrected quantitative identification method based on normalized Raman spectroscopy. The corresponding physical mechanisms, model applicability, error sources, comparative advantages as well as on-site feasibility are discussed in depth below.

4.1 Physical Mechanisms of Temperature Effects on Oil Droplet Distribution and Raman Signals

Experimental observations reveal that oil droplets in oil-containing drilling fluids are predominantly distributed in the range of 1000–5000μm^3, and this distribution is highly temperature-dependent. Physically, elevated temperature alters the interfacial tension between crude oil and the aqueous drilling fluid matrix, reduces fluid viscosity, and weakens the intermolecular interactions within the dispersion system, thereby affecting the coalescence, breakage and homogeneous dispersion of oil droplets. At a fixed temperature, higher crude oil concentration contributes to more uniform volume distribution of oil droplets, which can be attributed to the enhanced phase stability and suppressed local aggregation under sufficient oil-phase proportion.

Such micro-distribution variations further impose significant impacts on Raman scattering signals. On the one hand, temperature modulates the molecular vibration modes of crude oil and functional groups in the drilling fluid, leading to an observable peak shift near 3500cm^{-1} induced by O-H bonds in the water-based system. On the other hand, temperature changes the apparent ratio and effective scattering volume of crude oil in drilling fluids, resulting in regular variations in Raman spectral intensity. In the range of 2000–3000cm^{-1}, the Raman spectrum of oil-containing drilling fluid gradually approaches that of pure crude oil with increasing oil concentration. Collectively, temperature acts as a key thermodynamic factor governing both the macroscopic dispersion state of oil droplets and the microscopic spectral response characteristics of the system.

4.2 Applicability Conditions and Error Sources of the Quantitative Model

In this work, a quantitative analysis method was developed based on spectral normalization, temperature correction and weighted linear spectral superposition. Combined with the linear correlation between Raman peak position and temperature established in this study, the proposed method enables quantitative determination of crude oil concentration in drilling fluids. Under laboratory-prepared sample conditions, the relative error between the calculated and actual mixing ratios was controlled within 1%, indicating satisfactory quantitative accuracy and reliability.

The proposed method is applicable under the following conditions: (1) the composition of the drilling fluid matrix is relatively stable and its background spectrum can be reliably obtained; (2) the content of unknown impurities and interfering additives is sufficiently low so as not to overwhelm the characteristic peaks of crude oil; (3) the ambient temperature is within the simulated range ($\leq$ 85°C, corresponding to approximately 3000m burial depth), where Raman peak position varies linearly with temperature; and (4) the crude oil concentration is within the experimentally calibrated range without

severe phase inversion or abnormal aggregation.

The main error sources include: (1) slight deviation from the linear temperature-response relationship at elevated temperatures, leading to mildly increased prediction errors; (2) unpredictable background interferences from unidentified additives, mineral cuttings and solid particles in real drilling environments; (3) signal fluctuations caused by inhomogeneous oil droplet distribution and inconsistent local sampling volumes; and (4) weak spectral superposition between O-H groups of the water base and hydrocarbon vibration bands of crude oil.

4.3 Comparative Advantages Over Conventional Detection Methods

Compared with traditional hydrocarbon detection approaches utilized in petroleum engineering, the Raman-based quantitative method proposed herein exhibits prominent superiorities. First, it enables real-time and rapid detection without complex sample pretreatment, which is highly compatible with the requirements of LWD. Second, by means of spectral normalization and background subtraction, the method effectively distinguishes target oil signals from the drilling fluid matrix, showing stronger anti-interference capability than conventional semi-quantitative spectral techniques. Third, the quantitative accuracy with relative error $< 1\%$ is significantly higher than that of most on-site rapid detection methods. Fourth, the proposed method maintains excellent stability and effectiveness at simulated formation temperatures up to 85 °C, showing good adaptability to medium-deep well environments. Unlike traditional chemical assays and offline laboratory techniques, the Raman-based approach allows in-situ, continuous, and non-destructive monitoring, which is essential for real-time reservoir evaluation during drilling.

4.4 Feasibility and Limitations in Practical Drilling Scenarios

Experimental results verify the feasibility of applying Raman spectroscopy to on-line hydrocarbon detection in oil-containing drilling fluids under simulated downhole conditions. Characteristic Raman peaks of crude oil can be clearly identified even at 85°C, suggesting that the developed approach can be integrated into downhole logging tools for real-time monitoring of drilling fluid hydrocarbon content, with the signal stability is barely affected by crude oil concentration but mainly regulated by temperature. These results support the practical potential of Raman-based devices for in-situ, rapid and accurate hydrocarbon identification during drilling.

Nevertheless, several limitations must be acknowledged for field applications. Firstly, this study was conducted using clean, laboratory-prepared samples, whereas actual drilling fluids contain complex additives, solid weighting materials, rock cuttings and various unknown impurities, which may distort the background spectrum and interfere with peak recognition. Secondly, the current model is established under atmospheric pressure and linear temperature assumption; its performance under high-pressure and ultra-high-temperature downhole conditions remains to be verified. Thirdly, practical challenges such as probe contamination, fluid turbulence, gas bubble interference and downhole vibration may degrade spectral quality and detection repeatability. Finally, since crude oil concentration only induces a fluctuation of Raman peak intensity within 30–100, the intrinsic response sensitivity is relatively limited, which may restrict its performance in detecting extremely low oil content.

5 Conclusions

This study simulates the formation temperature gradient under normal pressure to observe crude oil distribution in oil-containing drilling fluids and analyze its Raman spectral characteristics. A quantitative analysis formula for identifying crude oil in drilling fluids is proposed, and the following conclusions are drawn:

1. The distribution of oil droplets in oil-containing drilling fluid is concentrated between 1000-5000 μm^3 and is significantly influenced by temperature. Higher crude oil concentration results in a more even volume distribution of oil droplets.

2. Raman spectra comparison shows that oil-containing drilling fluid shifts left at 3500cm^{-1}, and its peaks at 1000-3000cm^{-1} align with crude oil. At higher crude oil concentrations, the Raman spectrum increasingly resembles that of crude oil. Temperature affects the visual area ratio of crude oil, influencing Raman intensity. The concentration of crude oil has minimal impact on the Raman spectrum.

3. A weighted sum equation, based on normalized Raman peaks, quantitatively identifies crude oil

concentration in the drilling fluid. The error between calculated and actual ratios is less than 1%, with a slight increase in error as temperature rises.

4. The experiment demonstrates that hydrocarbon detection equipment can accurately detect crude oil in oily drilling fluids in real time during drilling. Even when simulating a 3000 m deep formation with a maximum temperature of 85 °C, the Raman peaks of crude oil can still be identified.

This confirms Raman spectroscopy as a real-time, fast, and accurate tool for hydrocarbon detection in drilling fluid, deserving further research for drilling detection equipment.

Data Availability Statement

Data will be made available on request.

Funding

This work was supported in part by the National Natural Science Foundation of China under Grant 42502155; in part by the Applied Basic Research Program of Liaoning Provincial Science and Technology Department under Grant 2023JH2/101300223; in part by the Basic scientific research project of Liaoning Provincial Department of Education under Grant LJ212410148053; in part by the Innovation Team Project of Liaoning Petrochemical University under Grant LX2024001; in part by the Liaoning Provincial Science and Technology Joint Program (Key Research and Development Program) under Grant 2025JH2/101800078.

Conflicts of Interest

The authors declare no conflicts of interest.

AI Use Statement

The authors declare that no generative AI was used in the preparation of this manuscript.

Ethical Approval and Consent to Participate

Not applicable.

References

[1] Sviridov, M., Belyaeva, O., Podberezhnyy, M., Zverev, V., Mosin, A., & Antonov, Y. (2018). First application of logging-while-drilling deep-azimuthal resistivity tool and advanced data-interpretation software for reservoir navigation at west salym field in Russia. *SPE Reservoir Evaluation & Engineering, 21*(03), 593-608. [CrossRef]

[2] Tan, B., Zhang, K., Su, Y., Li, S., & Zhang, L. (2022). Research on acoustic logging while drilling transmitting technologies. *Journal of Geophysics and Engineering, 19*(3), 511-520. [CrossRef]

[3] Ge, Y., Luo, Q., Chen, H., & Wang, J. (2022). A new porosity evaluation parameter based on neutron porosity logging. *Applied Radiation and Isotopes, 190*, 110481. [CrossRef]

[4] Luycx, M., & Torres-Verdín, C. (2018). Rapid forward modeling of logging-while-drilling neutron-gamma density measurements. *Geophysics, 83*(6), D231-D246. [CrossRef]

[5] Jain, V., Saumya, S., Vij, J., Singh, J., Singh, B., Pattnaik, S., ... & Collett, T. S. (2019). New technique for accurate porosity estimation from logging-while-drilling nuclear magnetic resonance data, NGHP-02 expedition, offshore, India. *Marine and Petroleum Geology, 108*, 570-580. [CrossRef]

[6] Liang, H., & Liu, G. (2022). Research on quantitative analysis method of PLS hydrocarbon gas infrared spectroscopy based on net signal analysis and density peak clustering. *Measurement, 188*, 110392. [CrossRef]

[7] Hashemi-Nasab, F. S., & Parastar, H. (2020). Pattern recognition analysis of gas chromatographic and infrared spectroscopic fingerprints of crude oil for source identification. *Microchemical Journal, 153*, 104326. [CrossRef]

[8] Li, Z., Pang, W., Liang, H., Chen, G., Ni, P., Duan, H., & Jiang, C. (2022). A novel method to realize multicomponent infrared spectroscopy gas logging based on PSO-split peak fitting-SVM. *Journal of Natural Gas Science and Engineering, 101*, 104496. [CrossRef]

[9] Liang, H., Liu, G., Zhongbing, L., & Ren, W. (2023). Improved SVR based on CARS and BAS for hydrocarbon concentration detection. *Vibrational Spectroscopy, 125*, 103494. [CrossRef]

[10] Liang, H., Chen, H., Guo, J., & Zuo, X. (2022). Detection and identification method of drilling total hydrocarbon gas based on infrared spectroscopy and KL+ BP-RBF algorithm. *IEEE Transactions on Instrumentation and Measurement, 71*, 1-10. [CrossRef]

[11] Blomberg, J., Schoenmakers, P. J., & Brinkman, U. A. T. (2002). Gas chromatographic methods for oil analysis. *Journal of Chromatography A, 972*(2), 137-173. [CrossRef]

[12] Wang, G., & Wang, Y. (2021, May). Qualitative Analysis and Quantitative Calculation of Crude Oil Drilling Fluid Mixtures Based on Raman Spectroscopy. In *2021 IEEE 10th Data Driven Control and Learning Systems Conference (DDCLS)* (pp. 1106-1111). IEEE. [CrossRef]

[13] Ying, G., Lian-Kui, D. A. I., Hua-Dong, Z., & others.

(2019). Quantitative analysis of main components of natural gas based on Raman spectroscopy. *Chinese Journal of Analytical Chemistry, 47*(1), 67-76. [CrossRef]

[14] Jianmei, L., Cunlei, L., Peng, G., & others. (2018). Identification method of crude oil in petroleum pipeline based on laser Raman detection technology. *Journal of Applied Optics, 39*(3), 436-441. [CrossRef]

[15] Larkin, P. (2017). *Infrared and Raman spectroscopy: principles and spectral interpretation*. Elsevier.

[16] Hannigan, J., Greig, F., Freeborn, S. S., & MacKenzie, H. A. (1999). A pulsed photoacoustic system for the spectroscopy and monitoring of hydrocarbon liquids using stimulated Raman scattering in a silica fibre as a near-infrared source. *Measurement Science and Technology, 10*(2), 93-99. [CrossRef]

[17] Mumm, A. S., & İnan, S. (2016). Microscale organic maturity determination of graptolites using Raman spectroscopy. *International Journal of Coal Geology, 162*, 96-107. [CrossRef]

[18] AlHumaidan, F. S., & Rana, M. S. (2021). Determination of asphaltene structural parameters by Raman spectroscopy. *Journal of Raman Spectroscopy, 52*(11), 1878-1891. [CrossRef]

[19] Miranda, A. M., Castilho-Almeida, E. W., Ferreira, E. H. M., Moreira, G. F., Achete, C. A., Armond, R. A., ... & Jorio, A. (2014). Line shape analysis of the Raman spectra from pure and mixed biofuels esters compounds. *Fuel, 115*, 118-125. [CrossRef]

[20] Wu, X., Lu, W., Ou, W., Caumon, M. C., & Dubessy, J. (2017). Temperature and salinity effects on the Raman scattering cross section of the water OH-stretching vibration band in NaCl aqueous solutions from 0 to 300 C. *Journal of Raman Spectroscopy, 48*(2), 314-322. [CrossRef]

[21] Kalasinsky, K. S., Minyard Jr, J. P., Kalasinsky, V. F., & Durig, J. R. (1989). Quantitative analysis of kerosines by Raman spectroscopy. *Energy & fuels, 3*(3), 304-307. [CrossRef]

[22] Pelletier, M. J. (2003). Quantitative analysis using Raman spectrometry. *Applied spectroscopy, 57*(1), 20A-42A. [CrossRef]

[23] Wang, M., Wang, J., Wang, P., Wang, Z., Tang, S., Qian, G., ... & Chen, W. (2025). Multi-pass cavity-enhanced Raman spectroscopy of complex natural gas components. *Analytica Chimica Acta, 1336*, 343463. [CrossRef]

[24] Wartewig, S. (2006). *IR and Raman spectroscopy: fundamental processing*. John Wiley & Sons. [CrossRef]

[25] Feng, Y., Zhang, T., Zhao, M., Zhang, X., Tang, H., & Sheng, Q. (2020). Raman-infrared spectral fusion combined with partial least squares (PLS) for quantitative analysis of polycyclic aromatic hydrocarbons in soil. *Analytical Methods, 12*(9), 1203-1211. [CrossRef]